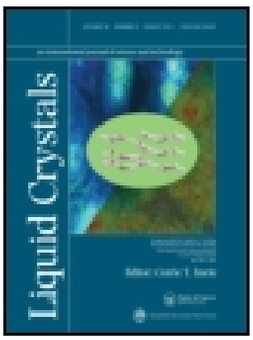

Liquid Crystals

ISSN: (Print) (Online) Journal homepage: https://www.tandfonline.com/loi/tlct20

Structural variants of *RM734* in the design of splay nematic materials

R. J. Mandle, S. J. Cowling & J. W. Goodby

To cite this article: R. J. Mandle, S. J. Cowling & J. W. Goodby (2021): Structural variants of *RM734* in the design of splay nematic materials, Liquid Crystals, DOI: 10.1080/02678292.2021.1934740

To link to this article: https://doi.org/10.1080/02678292.2021.1934740

LIQUID CRYSTALS
https://doi.org/10.1080/02678292.2021.1934740

Structural variants of *RM734* in the design of splay nematic materials

R. J. Mandle [a,b], S. J. Cowling [a] and J. W. Goodby[a]

[a]Department of Chemistry, University of York, York, UK; [b]School of Physics and Astronomy, University of Leeds, Leeds, UK

ABSTRACT

The recent discovery of the splay nematic phase, a new nematic polymorph that has been found to be both polar and ferroelectric, is the lead paragraph in an entirely new chapter in the history of liquid crystals. The potential for transformative applications utilising this state of matter – such as photonics, non-linear optics, memory applications and so on – can only be met with significant improvements in the temperature range of existing materials such as 4-(4-nitrophenoxycarbonyl) phenyl 4-methoxy-2-methoxybenzoate (*RM734*). Herein we present several families of materials which are structurally related to the archetypal new nematic material, *RM734*, including the first non-rod-like materials within the context of the splay nematic phase. We find that the incidence (or absence) of this new nematic variant in a designer material cannot be easily rationalised in terms of molecular dipole moment or polarisability. However, mixture formulation shows promise for the engineering of materials with improved working temperature ranges.

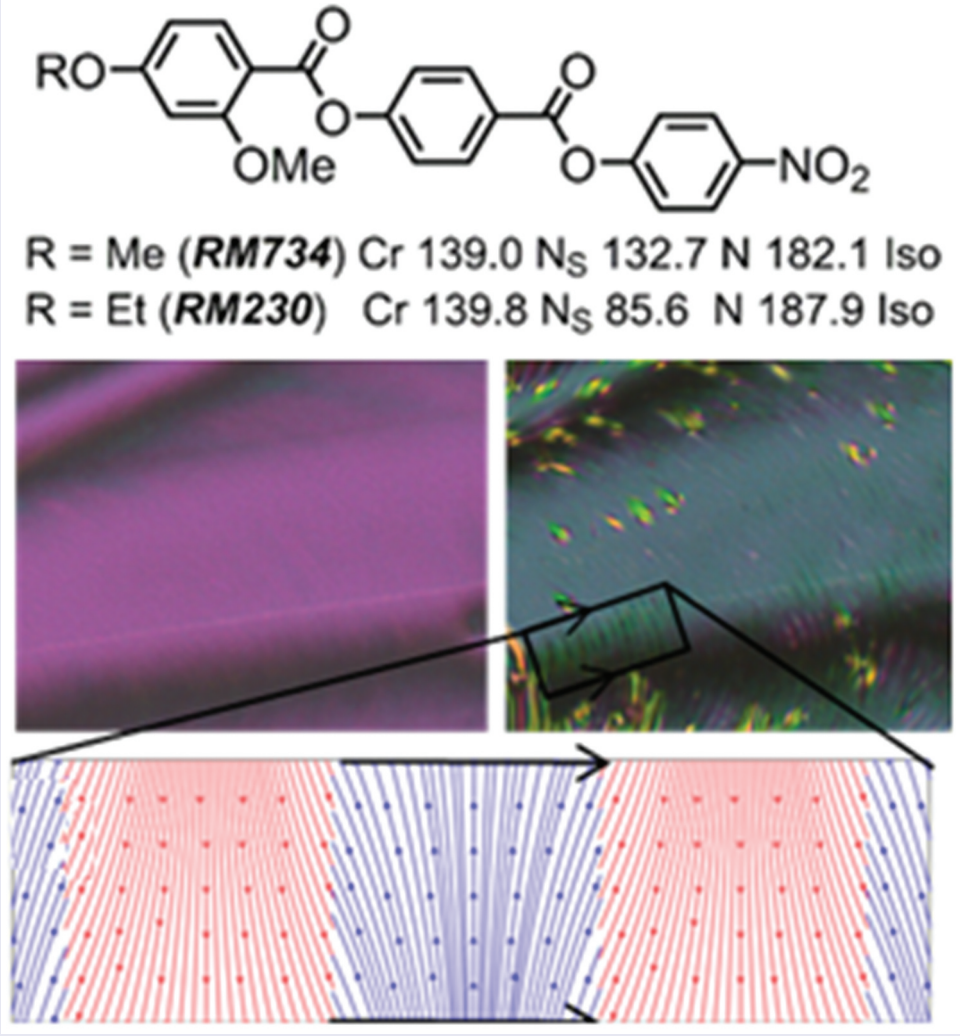

ARTICLE HISTORY
Received 23 March 2021
Accepted 22 May 2021

KEYWORDS
Liquid Crystals; Nematic; Splay Nematic; Ferroelectric Nematic; RM734

CONTACT R. J. Mandle r.mandle@leeds.ac.uk
Supplemental data for this article can be accessed here.

Introduction

As the uniaxial nematic liquid-crystalline state is widely employed in display technology, the discovery of new nematic ground states is met with great enthusiasm owing both to the extreme rarity of such phases, but also the possibility of transformative applications in displays and beyond [1]. For example, the prediction [2] and subsequent experimental discovery [3] of the twist-bend nematic phase has led to a resurgence of interest in liquid-crystalline dimers, with possible applications now emerging. The possibility of a ferroelectric nematic phase has been acknowledged for nearly a century [4,5]; the combination of ferroelectricity with nematic-like fluidity and ease of processing would have enormous potential for applications.

Early in 2017, we reported a rod-like material (*RM230*, Figure 1), first prepared many years earlier [6], with a large longitudinal electric dipole moment that exhibited two nematic phases separated by an enthalpic phase transition. At high temperatures, a conventional nematic phase was observed, and at lower temperatures a nematic phase of unknown structure, which we termed N_X [7]. Unfortunately, the monotropic N-N_X transition of *RM230* occurs almost 60°C below the melting point, and so detailed physical study on this material was impractical. Subsequently, in 2017 we published the first part of a larger body of work exploring how molecular features impact upon the then called N_X phase, identifying one material (*RM734*, Figure 1) as having transition temperatures which are better suited to detailed physical characterisation [8]. Later in the year, Nishikawa et al. reported on a rod-like material (named *DIO*), which exhibited two nematic phases, and possessed a giant dielectric anisotropy, shows ferroelectric properties, and exhibited similar optical textures to *RM230* [9].

Mertelj et al. revisited *RM734* in 2018, concluding that the lower temperature nematic phase is a splay modulated nematic phase (termed N_S), which is driven by an unusually small splay elastic constant approaching the phase transition [10]. The potential existence of a splay modulated nematic phase had been suggested many years earlier by Pleiner and Brand [11]. The N_S phase exhibits a periodic inhomogeneity in its optical texture parallel to the director, believed to be a splay modulation (Figure 1 (c, d)), with a period of ~9 microns [12]. In October 2019 Sebastian et al. demonstrated that the new N_S phase is comprised of polar domains with parallel dipole alignment, with the N-N_S transition having the characteristics of a ferroelectric phase transition, driving an orientational ferroelastic transition via flexoelectric coupling [12] and

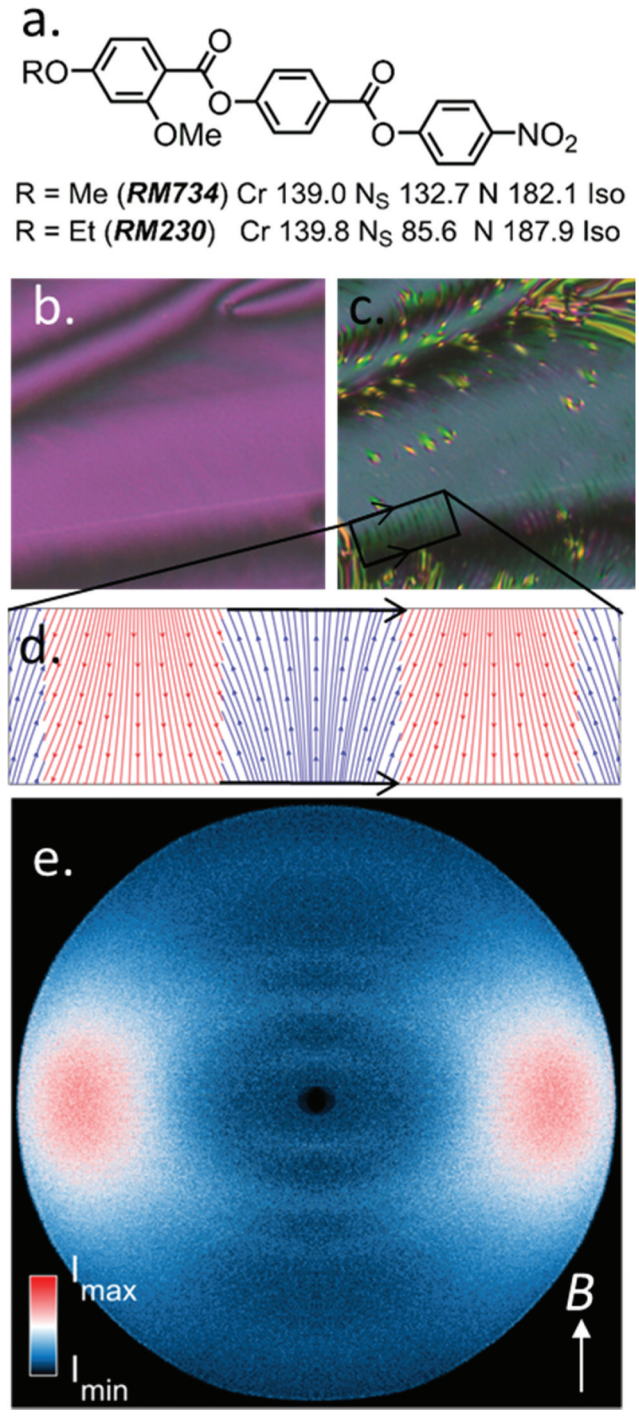

Figure 1. (a) Molecular structure and transition temperatures of two typical splay nematic materials; *RM230* (named **1** in ref [7]) and *RM734* (named **2** in ref [8]). Photomicrographs of (b) the nematic phase of *RM230* at 94.4°C, (c) the splay nematic phase of *RM230* at 76.4°C with modulations clearly visible; both (b) and (c) are of the same area of the sample; (d) idealised nematic director map for a periodic deformation according to the splay nematic model in ref [10]; (e) Background subtracted 2D SAXS pattern of a magnetically aligned sample of *RM230* in the N_S phase at 72°C; note the multiple diffuse peaks parallel to the magnetic field (*B*), and thus director.

is the first demonstration that the splay-nematic phase exhibited by *RM734* is ferroelectric [13].

RM734 and the N_S phase were later studied by others. In March 2020 Clark et al. made a first principle demonstration of the ferroelectric nature of the N_S phase which is reported to be homogenous (and so they called it N_F, for ferroelectric nematic, although it is not indicated if the transition is intrinsic or extrinsic for proper or improper ferroelectrics). Clark et al. find *RM734* to exhibit a giant spontaneous polarisation in the lower temperature nematic phase, saturating at ~6 μC cm^2 [14]. In November 2020 Aya et al. also demonstrated the polar order and ferroelectricity of the lower temperature nematic phase of *RM734* and other novel structurally related materials, noting that the lower temperature nematic is not homogenous as suggested in the N_F model [15]. Aya et al. suggest the name PN (for polar nematic), and demonstrate that the lower temperature nematic phase first observed in *RM230* is the same as that exhibited by Nishikawa. Interest in this area is growing rapidly: Manabe et al. have recently reported a material that exhibits a transition directly from the isotropic to ferroelectric nematic phase (Nf) [16], and Jakli et al. have reported a material (RT11001) which exhibits multiple ferroelectric nematic phases (F1, F2, F3) and displays an even larger spontaneous polarisation than *RM734*, saturating at 6.9 μC cm^2 [17]. The nomenclature describing the $N_X/N_S/N_F$/PN/F1 phase is not the subject of this paper and is a matter for future study and debate. However, we note that mesophase nomenclature and classification of new mesophases have not to date been made based on physical properties (e.g. polar, ferroelectric), but rather on symmetry and structure (e.g. biaxial, cubatic, twist-bend). Using the term nematic for thread-like defects, and splay to refer to the elastic properties (specifically the near zero K_1 measured for *RM734*) and the modulated structure. The classification therefore is unequivocal, and so herein we will therefore refer to the lower-temperature nematic phase exhibited by *RM734* and its homologues as a splay nematic (N_S). We note that the majority of the literature already uses this term, and this description appears to us to be best supported by experimental evidence available to date. What is certain is that the discovery of the polar and ferroelectric N_S phase marks the beginning of a transformative new chapter in liquid crystal science, with distinct and technologically relevant electro-optical effects exhibited by this phase [18,19] presenting a significant motivation towards development of new materials [20]. In parallel, and complementary to ongoing experimental efforts, theoretical understanding of the splay nematic phase is advancing rapidly [21–25].

Herein, we explore further variations on the core structure of *RM734*, subsequent to the discovery of the Ns phase. In keeping with lessons learned thus far, we use only short aliphatic chains in conjunction with large electric dipole moments generated through the incorporation of one or more nitro groups.

Experimental

Starting materials were obtained from commercial suppliers and used without further purification unless noted otherwise, whereas solvents were purified by percolation through activated alumina prior to use. The materials were characterised by NMR (^1H and ^{13}C), ESI mass spectrometry and FT-IR. For the sake of brevity, experimental details (synthetic schemes and procedures, chemical characterisation, details of instrumentation used, computational methods) are provided in the accompanying ESI. Density functional theory electronic structure calculations were performed in Gaussian G09 revision D01 [26]; semi-empirical calculations were performed in MOPAC2016 [27].

Results and discussion

We begin by considering materials analogous in structure to *RM734*, but with a lateral hydroxyl group *in lieu* of the methoxy unit. We explore variations in the position of the lateral hydroxyl group, and prepare variants without any lateral substituent. Transition temperatures and associated enthalpies of transition are presented in Table 1.

The three parent materials of the series that lack any lateral substituent (**10, 11** and **12**) exhibit wide temperature range nematic phases, but lack the N_S phase seen for *RM230* and *RM734*. The inclusion of a lateral hydroxyl group has only a minimal effect on melting point, but depresses the clearing point with respect to the parent compounds significantly. Notably, compounds **1–3** all decompose upon heating beyond ~240°C and so accurate determination of T_{NI} was not possible for these materials. It should be noted that there are few examples where the orientation of the ester functionalities is inverted. However, for the parent materials, which lack lateral substituents, the analogous 'inverted ester' compounds have been reported and are known by the acronym DB_nONO_2, where n is the number of carbon atoms in the terminal chain. The DB_nONO_2 compounds exhibit incommensurate and re-entrant phase behaviours. Some materials, such as DB_9ONO_2, exhibit smectic antiphases in which there is a modulated structure within the layer plane [28]. As these materials

Table 1. Transition temperatures (°C) and associated enthalpies of transition [kJ mol^{-1}]. Values for *RM230, RM734*, **2**, and **11** were taken from Mandle et al. [8] Compound **10** was also reported independently of this study by Aya et al. [15] Monotropic transitions are shown in parenthesis ().

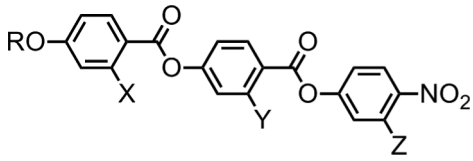

No.	R =	X =	Y =	Z =	Cr		N_S		N		Iso
RM734	Me	**OMe**	H	H	●	139.0 [34.8]	●	85.6 [0.2]	●	182.1 [0.6]	●
RM230	Et	**OMe**	H	H	●	139.8 [29.9]	●	132.7 [0.2]	●	187.9 [0.5]	●
1	Me	**OH**	H	H	●	209.6 [29.5]	-	-	●	240 Dec	
2	Et	**OH**	H	H	●	164.7 [39.4]	-	-	●	240 Dec	
3	Pr	**OH**	H	H	●	136.6 [35.4]	-	-	●	240 Dec	
4	Me	H	**OH**	H	●	205.3 [31.7]	-	-	(●	182.9 [0.6])	●
5	Et	H	**OH**	H	●	186.2 [35.3]	-	-	●	189.1 [0.4]	●
6	Pr	H	**OH**	H	●	166.4 [35.5]	-	-	●	190.3 [0.6]	●
7	Me	H	H	**OH**	●	162.5 [26.9]	-	-	(●	155.4 [0.7])	●
8	Et	H	H	**OH**	●	149.7 [27.0]	-	-	●	179.9 [0.4]	●
9	Pr	H	H	**OH**	●	137.0 [22.3]	-	-	●	197.4 [0.4]	●
10	Me	H	H	H	●	203.6 [42.9]	-	-	●	266.8 [0.7]	●
11	Et	H	H	H	●	155.2 [33.1]	-	-	●	276.4 [0.6]	●
12	Pr	H	H	H	●	148.3 [37.3]	-	-	●	274.8 [0.5]	●

were reported in the early 1980s, and hence well before the discovery of the Ns phase, we cannot say that this family does not exhibit splay nematic phases, but this possibility appears worthy of future investigation.

Compound **13**, a structural isomer of *RM230* in which the nitro group is in the *meta* position (Figure 2), is non-mesogenic (T_{MP} = 160.3°C, ΔH_{fus} = 27.1 kJ mol^{-1}). This demonstrates that position of the terminal nitro group is also critical to the observation of the splay nematic, and indeed the nematic, mesophase.

The N_S phase has to date only been observed in materials with large longitudinal dipole moments; how the molecular electric dipole varies with substitution pattern is therefore of interest. We calculated dipole moments and polarisabilities at the B3LYP-D3/6-31 G(d) level of DFT for the methoxy-terminated materials shown in Table 2. The dipole angle was computed as the angle between the dipole vector and the inertia tensor of the molecule in question. Compared

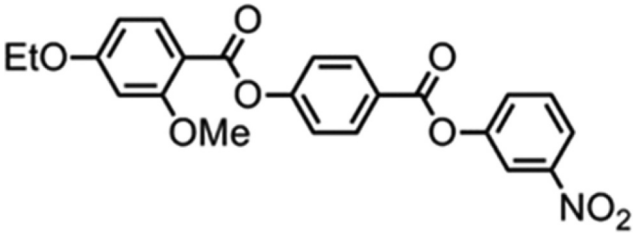

Figure 2. Molecular structure of compound **13**, T_{MP} = 160.3°C, ΔH_{fus} = 27.1 kJ mol^{-1}.

Table 2. Dipole moments (μ, Debye), dipole angle (β(μ), degrees), static anisotropic polarisability (Δα, Å^3) and static isotropic polarisability (α_{iso}, Å^3) of *RM734*, compounds **1, 4, 7, 10**, and **13**, calculated at the B3LYP-D3/6-31 G(d) level of DFT.

Cpd.	μ/D	β(μ)/°	Δα/Å^3	α_{iso}/Å^3
RM734	11.4	15.8	47.1	43.5
1	11.7	14.8	48.0	41.6
4	11.9	14.7	48.1	41.7
7	11.6	14.2	46.3	41.5
10	10.3	10.9	47.2	40.8
13	9.4	24.4	43.9	44.7

with the splay-nematic material *RM734*, the dipole moments of materials from Table 1 can be both smaller (e.g. **10, 13**) or larger (e.g. **1, 4**). Similarly, the incidence of the N_S phase does not appear to be only dependent upon the dipole angle, or polarisability values.

Although results to date suggest that the N_S phase is formed exclusively by molecules with extremely large electric dipole moments, dipole moments in isolation do not appear to be a particularly useful predictor for the incidence of the N_S phase. With this in mind, we next considered the role of the lateral unit in a series of 4-nitrobiphenyl benzoates (Table 3). These materials are analogous to *RM230*, but with only a single ester unit; this gave a modest reduction in the molecular electric dipole moment.

With respect to chemical stability, it was envisaged that the biphenyl-based materials would be more robust than their diester counterparts, and indeed we do not observe the decomposition that was noted for materials such as **1**–**3**. Although the majority of the nitrobiphenyl

Table 3. Transition temperatures (°C) and associated enthalpies [kJ mol^{-1}] for the 4-nitrobyphenylyl 2-alkoxy-4-ethoxybenzoates and 4-nitrobiphenyl 2-alkenyloxy-4-ethoxybenzoates. [1] Transition not observed by DSC. Values for **15** were taken from Mandle et al. [8] Monotropic transitions are shown in parenthesis ().

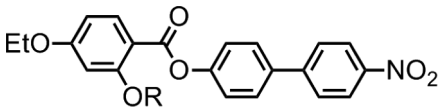

No.	R	Cr		N/N*		Iso
14	H	●	174.9 [24.7]	●	215.4 [0.6]	●
15	Me	●	151.6 [41.0]	●	165.9 [0.6]	●
16	Et	●	150.5 [29.7]	(●)	109.4) [1]	●
17	^{n}Pr	●	138.1 [20.1]	(●)	79.4 [0.6])	●
18	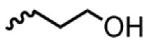	●	158.1 [27.0]	(●)	96.4) [1]	●
19	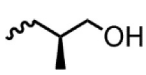	●	163.0 [34.3]	(●)	93.7) [1]	●
20	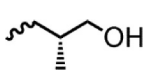	●	166.5 [33.7]	(●)	89.6) [1]	●
21	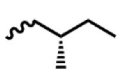	●	96.9 [28.6]	(●)	41.9 [1.1])	●
22		●	160.5 [49.9]	-	-	●

benzoate mesogens prepared exhibit nematic phases, none show splay nematic phases. The nematic phase of compound **17**, which has a lateral C3 chain, can be cooled to room temperature without formation of N_S or crystallisation, and so can be used to exclude the possibility that the N_S phase is obscured by crystallisation in this family of materials. For compound **21** a branched chiral alkoxy chain was used and this gives significantly lower melting points and clearing points compared to compound **17**. The inclusion of a terminal primary alcohol on the lateral C3 chain raises the onset temperature of the nematic phase significantly;

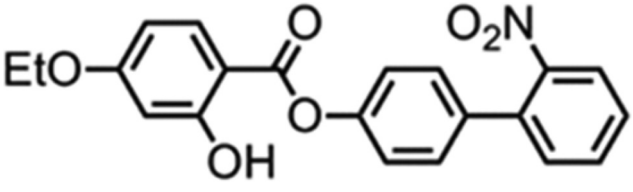

Figure 3. Molecular structure of compound **23**, T_{MP} = 131.8°C, ΔH_{fus} = 37.9 kJ mol^{-1}.

however, the material rapidly crystallises at this temperature; the same is true of the related branched chiral materials **19** and **20**. Compound **22** has a lateral allyl group and this material is non-mesogenic, melting and crystallising at a much higher temperature than the closely related compound **17**, which possesses a lateral propyloxy chain. However, the lateral allyloxy unit presents a handle for further synthetic transformations, as do the lateral hydroxyl groups of **18**–**20**. Compound **23** (Figure 3), a structural isomer of **14** in which the nitro group is in the *ortho* position, is non-mesogenic.

Removal of the lateral unit from compound **14**–**22**, to afford **24**, leads to a predictable rise in melting and clearing points. We sought to compensate for this by increasing the length of the terminal chain to propyloxy (**25**) or (S)-2-methylbutoxy (**26**); transition temperatures are presented in Table 4.

Although compounds **24** and **25** show wide temperature range nematic phases, the chiral compound **26** shows an additional smectic A phase. We do not observe even transient splay nematic phases in these materials. Two photomicrographs of the chiral nematic phase of compound **26** are given in Figure 4, showing the pseudo focal-conic defect texture obtained on cooling from the isotropic liquid, and a second showing the fingerprint texture obtained on heating of the smectic A phase into the chiral nematic phase. The absence of a lateral group leads to increased melting and clearing points when comparing compounds **24**–**26** with **14**–**22**.

As **26** exhibits a SmA phase and is also structurally related to *RM230*, we considered the possibility that binary mixtures could be formulated to generate materials with an N_S-SmA transition. This was motivated by a wish to study the behaviour of the elastic constants at the N_S-SmA transition, the structure of the resulting SmA phase and the possibility of re-entrant N_S phases. The binary phase diagram is shown in Figure 5. Unfortunately, the SmA and N_S phases of the respective materials are suppressed on moving across the phase diagram before we find a SmA-N_S transition temperature. At low concentrations of the chiral material **26** the N_S phase is retained. The behaviour of the first example of a chiral splay nematic phase (we suggest N_S* as a temporary abbreviation until the structure of this phase is elucidated) is distinct from the achiral phase and will be described at length in future papers. The monotropic nature of the 'N_S*' phase renders characterisation extremely challenging in this system. Nonetheless, we observe simultaneous micron scale periodic optical inhomogeneity reminiscent of the achiral N_S phase coupled with selective reflection of visible light (for other additives with large HTP), suggesting this to be a previously unobserved nematic-like phase with

Table 4. Transition temperatures (°C) and associated enthalpies [kJ mol^{-1}] of 4′-nitrobiphenylyl 4-alkoxybenzoates.

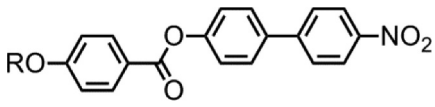

No.	R	Cr		SmA		N/N*		Iso
24	Et	●	162.6 [32.0]	-	-	●	276.0 [0.5]	●
25	Pr	●	144.1 [21.0]	-	-	●	218.3 [0.5]	●
26	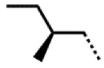	●	163.0 [15.1]	●	197.4 [0.2]	●	215.7 [0.3]	●

multiple distinct modulation periods, and perhaps the third distinct nematic phase variant discovered so far in the 21st century. Placing the mixture of *RM230*/**26** into a Cano Wedge cell with homeotropic alignment (to suppress the splay modulated structure), we observe Grandjean-Cano lines with a spacing (D) of ~300 µm which indicate a helical superstructure with pitch (P) of ~5.5 µm at 69°C. Studies into this new nematic variant are ongoing.

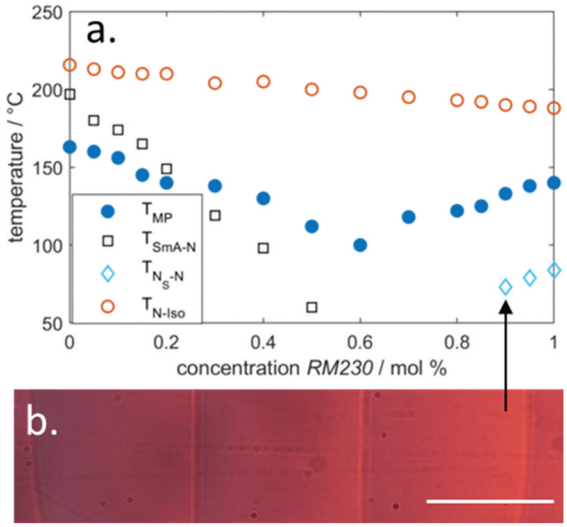

Figure 5. (a) Binary phase diagram for mixtures of *RM230* and **26**. (b) Photomicrograph of a mixture of 90 mol% of **26** in *RM230* (indicated with arrow) at 69°C in a Cano Wedge cell with homeotropic alignment and an inclination angle of tanα = 0.0092; pitch was calculated as P = 2.D.tanα. Scale bar = 250 µm.

We next sought to explore the possibility that multiple nitro groups could induce the formation of the N_S phase by increasing the molecular polarisability. Taking

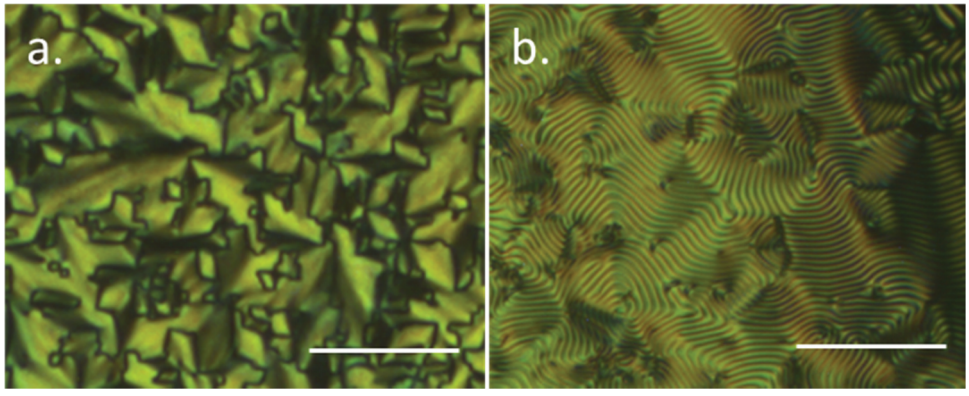

Figure 4. Pseudo focal-conic defect texture of the N* phase of **26** (a, 215°C) and the fingerprint texture of the N* phase of **26** (b, 199°C). In both images, the scale bar is 100 µm.

Table 5. Transition temperatures (°C), associated enthalpies [kJ mol^{-1}] and extrapolated virtual N – I transition temperature <°C> of polynitrated nitrobiphenyl benzoates. Monotropic transitions are shown in parenthesis ().

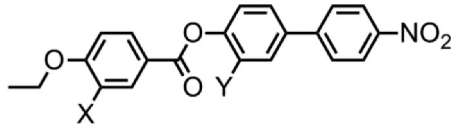

No	X	Y	Cr		N		I
24	H	H	●	162.6 [32.0]	●	276.0 [0.5]	●
27	NO_2	H	●	187.1 [24.8]	-	<138>	●
28	H	NO_2	●	160.5 [28.6]	(●	145.7 [0.5])	●

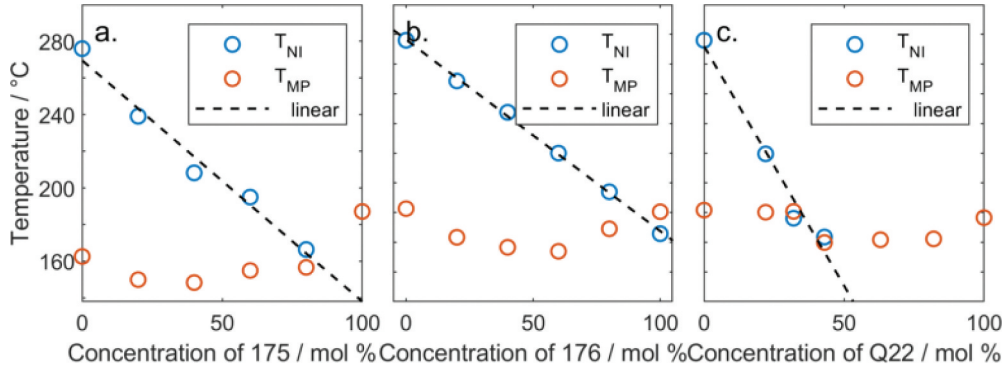

Figure 6. Transition temperatures (°C) of binary mixtures (mol%) of: (a) compounds **24/27**; (b) **24/28;** (c) **24/29**. For (a) and (c) the dashed line is a linear fit to T_{NI} versus concentration, which for **27** and **29** was used to obtain extrapolated isotropic to nematic transition temperatures of 138°C and −52.1°C, respectively.

compound **24** as our starting point, we prepared the di-nitrated analogues, **27** and **28** as shown in Table 5.

Whereas the mono-nitrated compound **24** exhibits a wide temperature range nematic phase, the introduction of a second nitro group in the first ring gives a non-mesogenic material. When a second nitro group is positioned in the middle ring of the molecule a small temperature range nematic phase is observed, albeit with a reduction of roughly 130 degrees in the clearing point. Thus, the introduction of a second nitro group in this position is detrimental to mesophase stability. However, when positioned in the opposing terminal ring the nematic phase is absent.

Consequently, the steric bulk of the second nitro group fails to confer any significant reductions in melting point over the parent material, owing to large increases in the transverse component of the dipole moment of the molecule; however, it does significantly suppress the clearing point. Binary mixtures of compounds **27** and **28** with compound **24** were prepared, and in the case of compound **27** this was used to extrapolate to give a virtual nematic to isotropic transition

Table 7. Melting point (°C) and associated enthalpy of fusion [kJ mol^{-1}] of compound **30.**

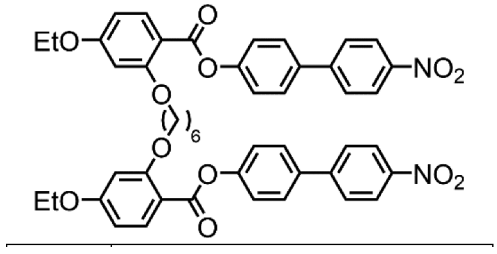

No.	Cr		I
30	●	207.4 [60.6]	●

Table 6. Melting point (°C), associated enthalpy [kJ mol^{-1}] for compound **29.**

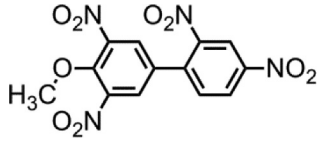

No.	Cr		I
29	●	154.7 [22.7]	●

temperature. The phase diagrams are presented in Figure 6.

We considered the possibility that additional nitro groups may affect beneficial reductions in melting point, remaining mindful of the hazards posed by polynitrated materials. With this in mind, we devised and prepared compound **29** (Table 6), which has sufficient nitro substituents to allow us to test this idea, yet too few to pose an explosion hazard. We find **29** to be non-mesogenic; further investigation *via* binary mixtures with compound **24** allowed us to extrapolate a virtual clearing point of −52.1°C for **29**.

We now turn briefly to the sculpting of more complex molecular arrangements, still inspired by *RM734*. Compound **30** is an H-shaped dimer, which can be considered as two molecules of **17** fused *via* a 1,6-dioxyhexamethylene linker, as shown in Table 7.

Comparison of **30** to its parent material (**17**) there is an increase in melting point of ~70°C. The monotropic nematic phase observed for **17** is absent in the dimer, **30**. The low solubility of **30** in both commercial nematics (5CB, E7) and also novel materials available in house (e.g. *RM734*, **24**) means we are unable to extrapolate a virtual T_{NI} for this material.

For an H-shaped dimer to exhibit nematic phases, one would anticipate an (anti)parallel alignment of the mesogenic units would be preferable; as **30** is

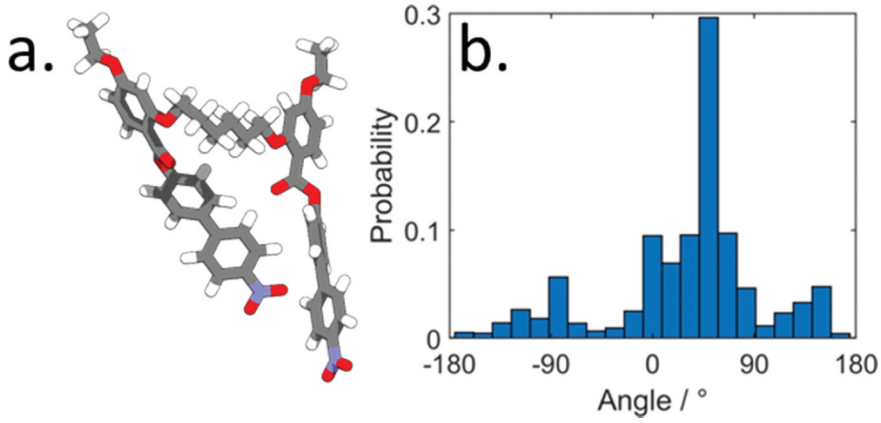

Figure 7. (a) Global energy minimum geometry of compound **30**, (b) histogram of energy as a function of the angle between the inertia axes of each mesogenic unit of **30** for a geometrically diverse conformer library.

Table 8. Melting point (°C) and associated enthalpy of fusion [kJ mol^{-1}] of compound **31.**

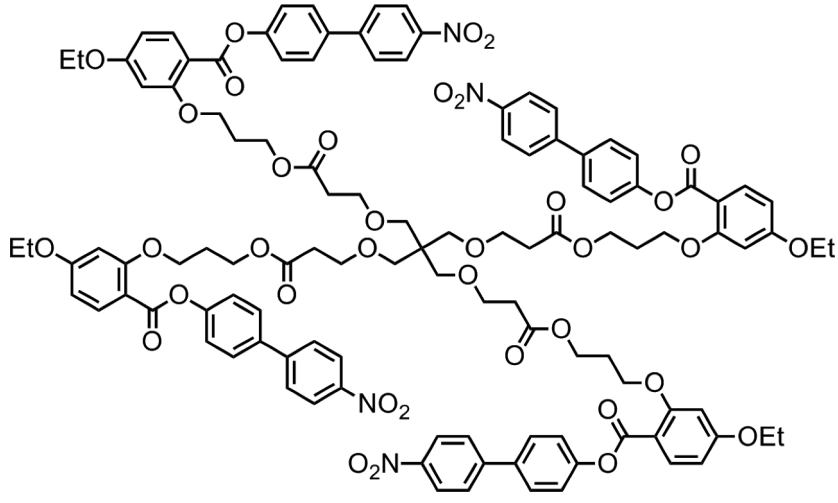

No.	Cr		I
31	●	55.8 [88.3]	●

non mesogenic we sought to study its molecular shape computationally. First, we obtained the global minimum energy geometry at the B3LYP/6-31 G(d) level of DFT. From this geometry we then generated a geometrically diverse conformer library (n = 5000) using a genetic algorithm to maximise the RMSD atom displacement [29]. Conjugate gradient geometry optimisations, using the PM7 semi-empirical method [27], were then performed for each conformer using MOPAC. We find that the global energy minimum geometry (single *gauche* in the central spacer) to have an angle of ~ 50° between the two mesogenic units; there is a broad distribution of populated angle (Figure 7), indicating **30** to have a globular shape which is evidently not especially conducive to forming nematic mesophases.

The tetrapodal compound **31** was formed *via* esterification of compound **18** with a tetracarboxylic acid derived from pentaerythritol (see Table 8). While this material met the design goal of reducing melting points compared to its parent, the splay nematic phase is absent and indeed the material, like the dimer, is non-mesogenic.

As with compound **30**, it is believed that the absence of mesomorphic behaviour in the supermolecule **31** is due to the alignment of the individual mesogenic units being unfavourable for the formation of a liquid crystal phase.

Mixture formulation

Traditional design of liquid crystal materials for use in electrooptic applications involves selection of central core units, appending terminal chains and the positioning of polar groups [30]. However, our studies show that the design of splay nematic materials is not so simple and requires delicate molecular sculpting. The usual approach to material design in such circumstances is to turn to formulation, and in the following, we describe our initial studies along this pathway.

Phase diagrams involving splay-nematic materials have to date displayed one of two behaviours: if both materials exhibit the N_S phase there is a near linear variation in $T_{Ns\text{-}N}$ as a function of concentration; if only one material displays the N_S phase in its neat state then it is readily suppressed in binary mixtures. Having developed a large number of '*RM734*-like' materials in this present work, we sought to explore ternary phase diagrams involving N_S materials. We prepared ternary mixtures of *RM230*, **2**, and **15**, evaluating transition temperatures by DSC and microscopy. In total, we evaluated 110 mixtures, and tabulated data is given in the ESI. Mirroring behaviour observed for binary mixtures, we find that for ternary mixtures with <80 mol% *RM230*, the N_S phase is absent, although below this concentration threshold it is generally retained. However, we find impressive reductions in melting point in the vicinity of the eutectic composition (minimum T_{MP} of 112°C at 0.47 mol% *RM230*, 0.29 mol% **2** and 0.24 mol% **15**).

Gratifyingly, we find that the Schröeder-van-Laar equation (see ESI, section 3) [31,32] is competent for predicting the melting points of the mixtures shown in Figure 8, while the clearing points are well described by a simple weight average of the 3 components.

This suggests that mixture formulation will be a viable route to improved temperature range splay nematics, although this will almost certainly require the synthesis of additional families of N_S materials so that a larger pool of compounds can be employed in mixture formulation.

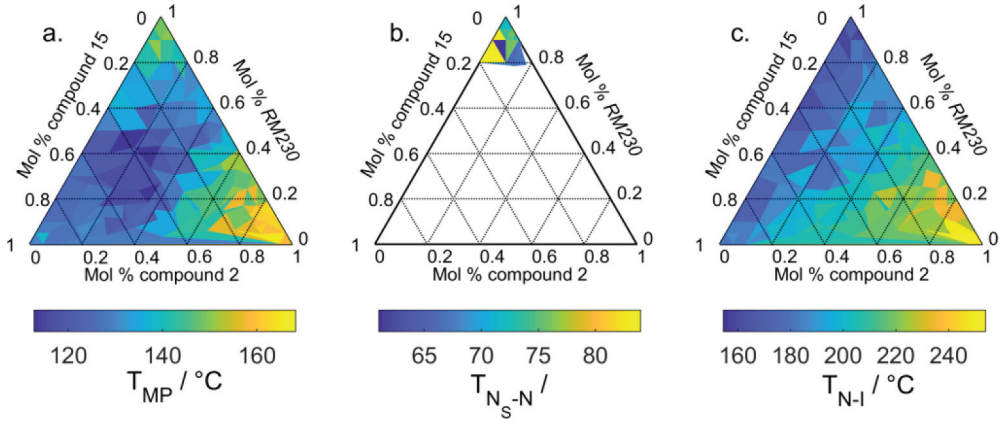

Figure 8. Experimental phase diagrams for ternary mixtures of *RM230*, **2** and **15**: (a) melting point; (b) N_s-N transition; (c) N-I transition. White regions in (b) correspond to areas where no N_S-N transition occurs, as judged by optical microscopy and DSC.

Conclusions

In the few years since our report of the first rod-like to exhibit a new nematic phase of matter in early 2017, these materials have since been shown to fulfil the promise of ferroelectric nematics over a century after such a phase was envisioned. While behaviour of these materials under applied electric fields is remarkable [19], the transformative applications potential of the ferroelectric splay nematic phase will only be realised should materials be designed that exhibit this phase over a suitable temperature range for applications use, most likely including ambient temperature. To this end, we report on a number of materials, which are structurally related to *RM734*, the archetypal N_S material. We find the N_S phase to be extremely sensitive to structural variations; removal of a single ester unit, or the lateral methoxy group from *RM734* prevents the formation of the splay nematic phase. We are unable to compensate for this with further structural modifications, such as increased aliphatic content or the use of more complex molecular architectures. Mixture formulation has the potential to offer significant reductions in melting point; however, the pool of N_S materials that are known is currently small and so there is limited scope for detailed formulation work presently.

The realisation a low molecular weight splay-nematic material at ambient temperature poses a significant challenge. Much like the quest for ambient temperature uniaxial nematics for display devices in the 1960s onwards, we do not view the present challenge as an intractable problem, but rather one that will yield under the application of sufficient synthetic effort allied with physical characterisation.

Acknowledgments

The authors thank Dr Charles Bradbury of the University of York for assistance with the synthesis of 4-nitroresorcinol and 4-hydroxy-4′-nitrobiphenyl. Raw data pertinent to this work are available *via* the University of York data catalogue.

Disclosure statement

No potential conflict of interest was reported by the author(s).

ORCID

R. J. Mandle http://orcid.org/0000-0001-9816-9661
S. J. Cowling http://orcid.org/0000-0002-4771-9886

References

[1] Lavrentovich OD. Ferroelectric nematic liquid crystal, a century in waiting. PNAS. 2020;117:14629–14631.
[2] Dozov I. On the spontaneous symmetry breaking in the mesophases of achiral banana-shaped molecules. Europhys Lett. 2001;56:247–253.
[3] Cestari M, Diez-Berart S, Dunmur DA, et al. Phase behavior and properties of the liquid-crystal dimer 1″,7″-bis(4-cyanobiphenyl-4′-yl) heptane: a twist-bend nematic liquid crystal. Phys Rev E Stat Nonlin Soft Matter Phys. 2011;84:031704.
[4] Debye P. Einige Resultate einer kinetischen Theorie der Isolatoren. Physikalische Zeitschrift. 1912;13:97–100.
[5] Born M. Über anisotrope Flüssigkeiten. Versuch einer Theorie der flüssigen Kristalle und des elektrischen Kerr-Effekts in Flüssigkeiten. Sitzungsber Preuss Akad Wiss. 1916;30:614–650.
[6] Mandle R. J., The Nitro Group in Liquid Crystals (PhD Thesis), University of York, York UK, 2013.
[7] Mandle RJ, Cowling SJ, Goodby JW. A nematic to nematic transformation exhibited by a rod-like liquid crystal. Phys Chem Chem Phys. 2017;19:11429–11435.
[8] Mandle RJ, Cowling SJ, Goodby JW. Rational design of rod-like liquid crystals exhibiting two nematic phases. Chemistry. 2017;23:14554–14562.
[9] Nishikawa H, Shiroshita K, Higuchi H, et al. A fluid liquid-crystal material with highly polar order. Adv Mater. 2017;29:29.
[10] Mertelj A, Cmok L, Sebastian N, et al. Splay nematic phase. Phys Rev X. 2018;8:041025.
[11] Pleiner H, Brand HR. Spontaneous splay phases in polar nematic liquid-crystals. Europhys Lett. 1989;9:243–249.
[12] Sebastián N, Cmok L, Mandle RJ, et al. Ferroelectric-ferroelastic phase transition in a nematic liquid crystal. Physical Review Letters. 2020;124:037801.
[13] Miller J. A novel liquid-crystal phase is ferroelectric. Phys Today. 2020;73:17–19.
[14] Chen X, Korblova E, Dong D, et al. First-principles experimental demonstration of ferroelectricity in a thermotropic nematic liquid crystal: polar domains and striking electro-optics. PNAS. 2020;117:14021–14031.
[15] Li J, Nishikawa H, Kougo J, et al. Development of polar nematic fluids with giant-\k{appa} dielectric properties. 2020 [cited 2020 Nov 01]. Available from: https://ui.adsabs.harvard.edu/abs/2020arXiv201114099L
[16] Manabe A, Bremer M, Kraska M. Ferroelectric nematic phase at and below room temperature. Liq Cryst. 2021;1–8. DOI:10.1080/02678292.2021.1921867
[17] Saha R, Nepal P, Feng C, et al. Multiple ferroelectric nematic phases of a highly polar liquid crystal compound. 2021 [cited 2021 Apr 01]. Available from: https://ui.adsabs.harvard.edu/abs/2021arXiv210406520S
[18] Chen X, Korblova E, Glaser MA, et al. Polar in-plane surface orientation of a ferroelectric nematic liquid crystal: polar monodomains and twisted state electro-optics. 2020 [cited 2021 Dec 01]. Available from: https://ui.adsabs.harvard.edu/abs/2020arXiv201215335C
[19] Sebastián N, Mandle RJ, Petelin A, et al. Electrooptics of mm-scale polar domains in the ferroelectric splay nematic phase. 2021 [cited 2021 Mar 01]. Available from: https://ui.adsabs.harvard.edu/abs/2021arXiv210310215S
[20] Mandle RJ, Sebastián N, Martinez-Perdiguero J, et al. On the molecular origins of the ferroelectric splay nematic phase. 2020 [cited 2020 Nov 01]. Available

from: https://ui.adsabs.harvard.edu/abs/2020arXiv201102722M
[21] Čopič M, Mertelj A. Q-tensor model of twist-bend and splay nematic phases. Phys Rev E. 2020;101:022704.
[22] Chaturvedi N, Kamien RD. Gnomonious projections for bend-free textures: thoughts on the splay-twist phase. Proc R Soc Lond. 2020;476:20190824.
[23] Rosseto MP, Selinger JV. Theory of the splay nematic phase: single versus double splay. Phys Rev E. 2020;101:052707.
[24] Chaturvedi N, Kamien RD. Mechanisms to splay-bend nematic phases. Phys Rev E. 2019;100:022704.
[25] Kats EI. Stability of the uniform ferroelectric nematic phase. Phys Rev E. 2021;103:012704.
[26] Frisch MJ, Trucks GW, Schlegel HB, et al.Gaussian 09 revision d01. Gaussian, Inc., Wallingford CT, 2009.
[27] Stewart JJ. Optimization of parameters for semiempirical methods VI: more modifications to the NDDO approximations and re-optimization of parameters. J Mol Model. 2013;19:1–32. Epub 2012/ 11/29.
[28] Fontes E, Heiney PA, Haseltine JL, et al. High resolution X-ray scattering study of the multiply reentrant polar mesogen DB9ONO2. J. Phys. France.1986;47:1533–1539. DOI:10.1051/jphys:019860047090153300.
[29] O'Boyle NM, Banck M, James CA, et al. Open Babel: an open chemical toolbox. J Cheminform. 2011;3:33. Epub 2011/ 10/11.
[30] Goodby JW. The nanoscale engineering of nematic liquid crystals for displays. Liq Cryst. 2011;38:1363–1387.
[31] Hsu ECH, Johnson JF. Order and flow in mesophases .34. Phase-diagrams of binary nematic mesophase systems. Mol Cryst Liq Cryst. 1973;20:177–190.
[32] Hulme DS, Raynes EP. Eutectic mixtures of nematic 4′-substituted 4-cyanobiphenyls. J Chem Soc Chem Commun. 1974;98–99. DOI:10.1039/C39740000098